Nanotechnology 26 (2015) 455701 (8pp) doi:10.1088/0957-4484/26/45/455701

Visibility of atomically-thin layered materials buried in silicon dioxide

Ergun Simsek and Bablu Mukherjee

Department of Electrical and Computer Engineering, School of Engineering and Applied Science, The George Washington University, Washington, DC 20052, USA

E-mail: simsek@gwu.edu

Received 22 July 2015, revised 1 September 2015
Accepted for publication 7 September 2015
Published 16 October 2015

Abstract

Recently, the coating of thin oxide or nitride film on top of crystals of atomically-thin layered material (ATLM) has been introduced, which benefits optical and electrical properties of the materials and shields them from environmental contact, and has important implications for optoelectronics applications of layered materials. By calculating the reflection contrast, we show the possibility of using an additional oxide film on top of ATLM with good average optical color contrast in broad- and narrow-band wavelength ranges. Our work presents a more comprehensive map of optical color contrast of various ATLMs including graphene, MoS_2, $MoSe_2$, WS_2, and WSe_2 when kept in a sandwich structure between two thin SiO_2 films on a Si substrate. The average color contrasts of ATLMs with varying thicknesses of SiO_2 films at three different wavelength ranges (i.e. broadband range, range for green filtering and range for red filtering) have been discussed with a summary of optimized thicknesses of the top and bottom oxide films in order to achieve the highest color contrast from the sandwich structures.

S Online supplementary data available from stacks.iop.org/NANO/26/455701/mmedia

Keywords: 2D layered materials, nanosheets, optical contrast, reflectivity

(Some figures may appear in colour only in the online journal)

Introduction

Two dimensional (2D) atomically-thin layered materials (ATMLs) including graphene, molybdenum disulphide (MoS_2), molybdenum diselenide ($MoSe_2$), tungsten disulfide (WS_2), and tungsten diselenide (WSe_2), with thicknesses of mono-, bi-, tri- and few-layers, have attracted great interest due to their unique electrical, optical and mechanical properties [1]. One of many parameters that affects these properties is the thickness of these layered materials (LMs). Many methods, including Raman spectroscopy [1, 2], atomic force microscopy (AFM) [1, 3] and optical imaging [4–8] have been employed to identify the thickness of the 2D materials, which is important in the scientific research and application communities. Optical imaging offers the possibilities of simple, rapid and non-destructive characterization of ATLM [4–8]. The optical color contrast is an important observation to locate ATLM with respect to the interface color of the underlying oxide layer. Enhancing the color contrast of LM contributes additional help to fundamental research. The color contrast in various ATLM systems including graphene [4, 9, 10], MoS_2 [5, 11], and WSe_2 [12] has been studied by varying the underlying oxide layer thickness. Good color contrast for different types of ATLM under different geometries is important in order to determine the optimal imaging condition for their optical detection.

Various methods have been devoted to improving the color contrast, including the selection of substrate [5], selection of light illumination [4, 5], ratio of color difference [13], and usage of reflection and color spectroscopy [14], etc. It has been shown experimentally and numerically that modulating the thicknesses of oxide layer of underlying substrate [5] and capping oxide [12] layers can significantly enhance the light absorption and emission properties of ATLMs. The dielectric surroundings around an ATLM can optically modulate the reflected light intensity under light illumination [15, 16]. Thus the capping oxide layer plays an important role in engineering light coupling in ATLMs. On the other hand, coating ATLMs with silicon dioxide (SiO_2) or Si_xN_y improves mechanical coupling of the LM with surrounding dielectrics [17]. Capping of an oxide film on a LM may further enhance device stability, performance, and protect from environmental contact [18, 19]. Zhang *et al* recently reported results of optical contrast spectra on crystalline monolayer MoS_2 material by improving the spatial resolution of a reflectance spectrum via spatial filtering [11]. In the past, substrate interference has been used to quantify the thickness of SiO_2 film grown on a Si substrate by studying the reflection color contrast [20]. Similar strategies have also been employed on ATLM systems to identify the thickness using color contrast under optical microscopy [9]. Commonly, a Si substrate coated with a ~90 nm and ~285 nm SiO_2 layer corresponding to the most constructive and destructive substrate, respectively, are used for ATLM to obtain a high color contrast. Considering graphene's almost constant refractive index in the visible range of the electromagnetic spectrum, one can roughly estimate the optimum thickness of the oxide using $d(\lambda, i) = (2i - 1) \times \lambda / 4n_{ox}$, where λ is wavelength, n_{ox} is refractive index of the oxide and i is a positive integer. For example, at a wavelength of 580 nm, the first two optimum thicknesses are 95 and 285 nm when $n_{ox} = 1.54$, which is the refractive index of SiO_2 at this particular wavelength. These numbers are very close to the industry standards. However, a similar approach cannot be implemented for transition metal dichalcogenides because of their highly dispersive nature [22–24, 26–28]. Further, if we add another oxide layer on top, the situation becomes even more complicated and one cannot estimate the optimum thickness without taking dispersion, reflections, and transmissions into account.

In this report, we calculate the average color contrast of various ATLMs deposited on a SiO_2/Si substrate with a thin coating of SiO_2 film using wavelength-dependent refractive indices for each material. We find that the thickness of the capping oxide should not exceed 60 nm (in some cases 40 nm) and in fact the optimum value can be determined as a function of wavelength and the thickness of the oxide between the ATLM and Si substrate. Our report summarizes the required thicknesses of underlying and capping SiO_2 layers in a sandwich structure geometry of $SiO_2/ATLM/SiO_2/Si$ substrate to obtain the best average color contrast at different wavelength ranges, i.e. broadband range (400–750 nm), green filtering range (500–560 nm) and red filtering range (600–660 nm), The provided theoretical results are expected to be very useful as a benchmark in future studies with such sandwich structures.

Theory and numerical results

A schematic of the sandwich geometry of $SiO_2/ATLM/SiO_2$ on a Si substrate is shown in figure 1(a). In order to calculate the optical contrast, we use a SiO_2-coated Si substrate as schematically shown in figure 1(b), where the thickness of the SiO_2 layer is the sum of the capping and underlying oxide layers' thicknesses. For both geometries, the reflected light intensities are calculated from the top of the structures.

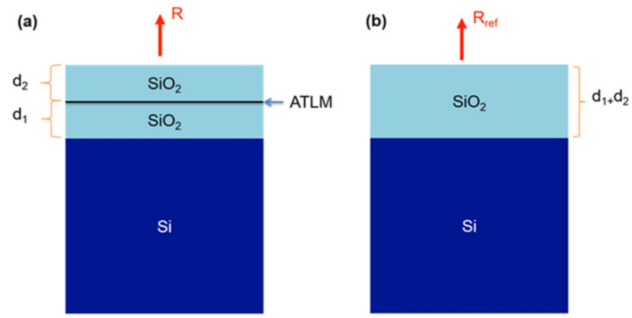

Figure 1. (a) The geometry under examination: an ATLM-coated SiO_2/Si substrate covered with another SiO_2 layer. The thicknesses of the SiO_2 layers under and above the ATLM are d_1 and d_2, respectively; (b) the reference geometry used to calculate the contrast.

In order to obtain more realistic results, we use wavelength-dependent refractive index formulas for each material (table S1). For graphene, the closed form expression developed in [21] is used, assuming a hopping parameter of 2.7 eV. The refractive indices of MoS_2 from [22–26], $MoSe_2$ from [22, 26], WS_2 from [22, 25, 27] and WSe_2 from [22, 26, 28] are used for comparison. Within the implementation of [23], we assume room temperature and zero Fermi energy. The indices for Si and SiO_2 are taken from [29] and [30], respectively. The thickness of graphene is assumed to be 0.335 nm, whereas monolayer transition metal dichalcogenides (TMDCs) are assumed to be 0.7 nm thick.

The reflectance of the substrates is calculated using the wave propagation in layered media formulation [31] implemented in MATLAB. The first set of substrates has four layers: infinitely thick Si, first SiO_2 layer (i.e. underlying) with a thickness of d_1, ATLM, and the second SiO_2 layer (i.e. capping) with a thickness of d_2. The second set of substrates, which is used as a reference, has only two layers: an infinitely thick Si layer and a SiO_2 layer with a thickness of $d_1 + d_2$. The contrast (C) is defined as the relative intensity of reflected light in the presence (R) and absence (R_{ref}) of ATLM and can be written as:

$$C(\lambda_i) = \frac{R_{ref}(\lambda_i) - R(\lambda_i)}{R_{ref}(\lambda_i)}, \quad (1)$$

where λ_i is the ith wavelength sample chosen over a finite range between λ_{min} and λ_{max}, such that $\lambda_i = \lambda_{min} + (i - 1)(\lambda_{max} - \lambda_{min})/(N - 1)$ and $i = 1, 2, 3, \ldots, N$.

In order to verify the accuracy of our implementation model, we first analyze ATLM-coated SiO_2/Si substrates by setting $d_2 = 0$. Figure 2(a) shows the contrast as a function of incident wavelength and SiO_2 thickness for graphene. The result shows a similar trend to the results found in the literature [4] for graphene. Briefly, in [4], the researchers suggest 90 nm and 280 nm are the optimum SiO_2 thickness values while working around green light and slightly higher values in white light, respectively, to increase the visibility of graphene. Considering the fact that they use constant refractive indices over the entire spectrum and here we fully take dispersion into account, our calculations suggest slightly

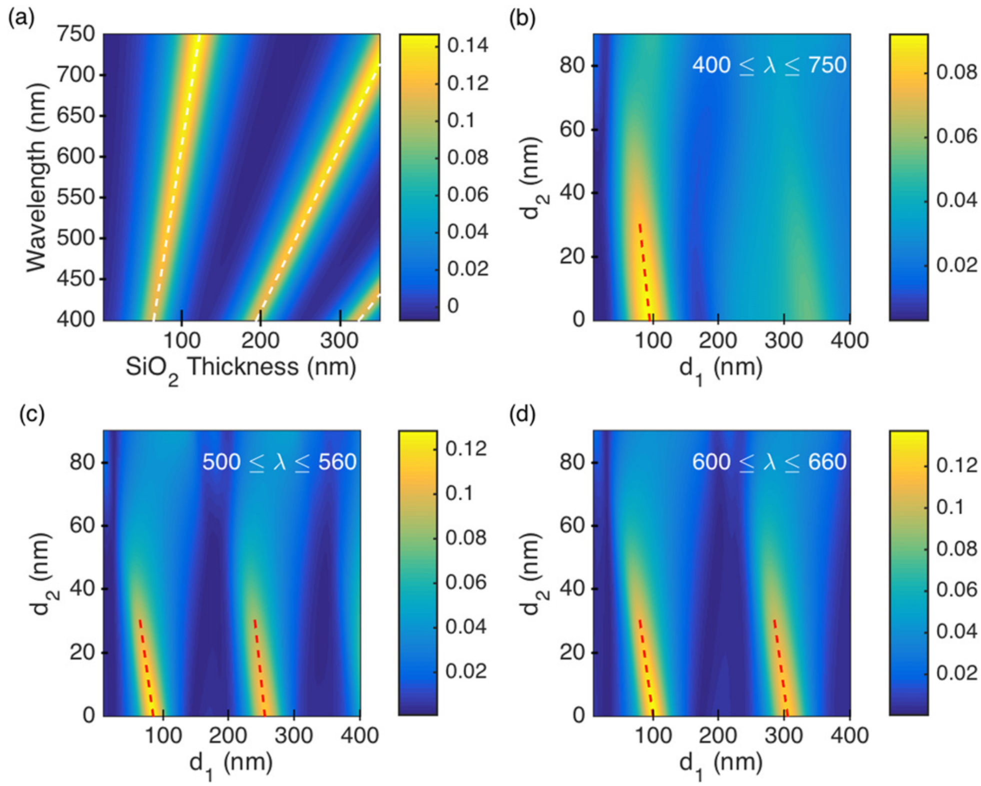

Figure 2. For graphene analysis: (a) color plot of the contrast as a function of wavelength and SiO_2 thickness; white dashed lines show $d(\lambda, i) = (2i - 1)\lambda/4n_{SiO2}$ for $i = 1$, 2, and 3. (b)–(d) Average color contrast as a function of d_1 and d_2 for three different wavelength regions. The color scale on the right shows the expected contrast. The red dashed lines highlight where the contrasts are local maxima.

different oxide thicknesses: 95 nm for white light; 85 nm and 255 nm for the green light region; and 100 nm and 305 nm for the red light region.

Next we analyze the graphene buried in SiO_2 in a sandwich structure geometry as follows. We treat the substrate as a four-layer medium where the thicknesses of the SiO_2 layers, d_1 and d_2, are the variables. In order to find the optimum d_2 as a function of d_1, we calculate the average contrast (C_{ave}) using the following equation (2).

$$C_{ave} = \frac{1}{N}\sum_{i=1}^{N} C(\lambda_i) \tag{2}$$

We first consider a broadband illumination, which is more applicable for practical applications with standard color cameras avoiding the need for additional color filters, and we calculate the average contrast over the whole visible range, i.e. $\lambda_{min} = 400$ nm, $\lambda_{max} = 750$ nm, and $N = 351$. Similar methodology is applied for the other two filtered colors of light (i.e. green and red) by selecting their appropriate wavelength range. Figures 2(b)–(d) plot average color contrast as a function of d_1 and d_2 for three different wavelength regions for graphene. As shown in figure 2, our calculations suggest that the thickness of the second SiO_2 layer, which is the capping oxide layer of thickness d_2, should always be smaller than 30 nm. For $0\text{ nm} \leqslant d_2 \leqslant 30$ nm cases, we also observe that the visibility of the graphene changes as we increase d_1, which should not be bigger than ~95 nm to obtain a good color contrast in the white light range. For the green and red light, we observe an additional region of (d_1, d_2) for good contrast. In this region, d_1 values are much higher (>240 nm) while d_2 still has to be less than or equal to 30 nm. In both regions, the bright spots in each figure of color contrast suggest that an optimum d_1 value can be calculated with the equation (3) as follows:

$$d_1 = \alpha d_2 + \beta, \tag{3}$$

where α is the slope of the dashed line passing through the bright spots and β is a positive number, which can be extracted from the figures of color contrast. For example, we suggest that d_2 should be something between 0 and 30 nm for graphene, and the optimum d_1 value can be calculated from $d_1 \approx 95 - 0.5d_2$, which is in the range of 80 to 95 nm for white light illumination. To give a numerical example, if $d_2 = 20$ nm, the optimum value of d_1 is 85 nm. Again by using this simple equation, we can conclude that if we are going to work with graphene growth on a Si wafer with ~90 nm thick SiO_2 layers and cover it with SiO_2, it should be 10 nm thick for the highest visibility under broadband illumination. For filtered cases, the suggested d_1 ranges and the equations to calculate the optimum d_1 values are listed in table 1.

Next we use our model to analyze average color contrast of monolayer MoS_2 as a function of SiO_2 thickness in the geometry of $MoS_2/SiO_2/Si$ substrate for three different

Table 1. Underlying oxide thickness ranges at three different wavelength regions for graphene. The thickness of the capping should be less than or equal to 30 nm.

	White Light $400 \leqslant \lambda \leqslant 750$ nm	Green Light $500 \leqslant \lambda \leqslant 560$ nm		Red Light $600 \leqslant \lambda \leqslant 660$ nm	
Graphene	$d_1 \approx 95 - 0.5d_2$ $80 \leqslant d_1 \leqslant 95$ nm	$d_1 \approx 85 - 0.67d_2$ $65 \leqslant d_1 \leqslant 85$ nm	$d_1 \approx 255 - 0.5d_2$ $240 \leqslant d_1 \leqslant 255$ nm	$d_1 \approx 100 - 0.67d_2$ $80 \leqslant d_1 \leqslant 100$ nm	$d_1 \approx 305 - 0.67d_2$ $285 \leqslant d_1 \leqslant 305$ nm

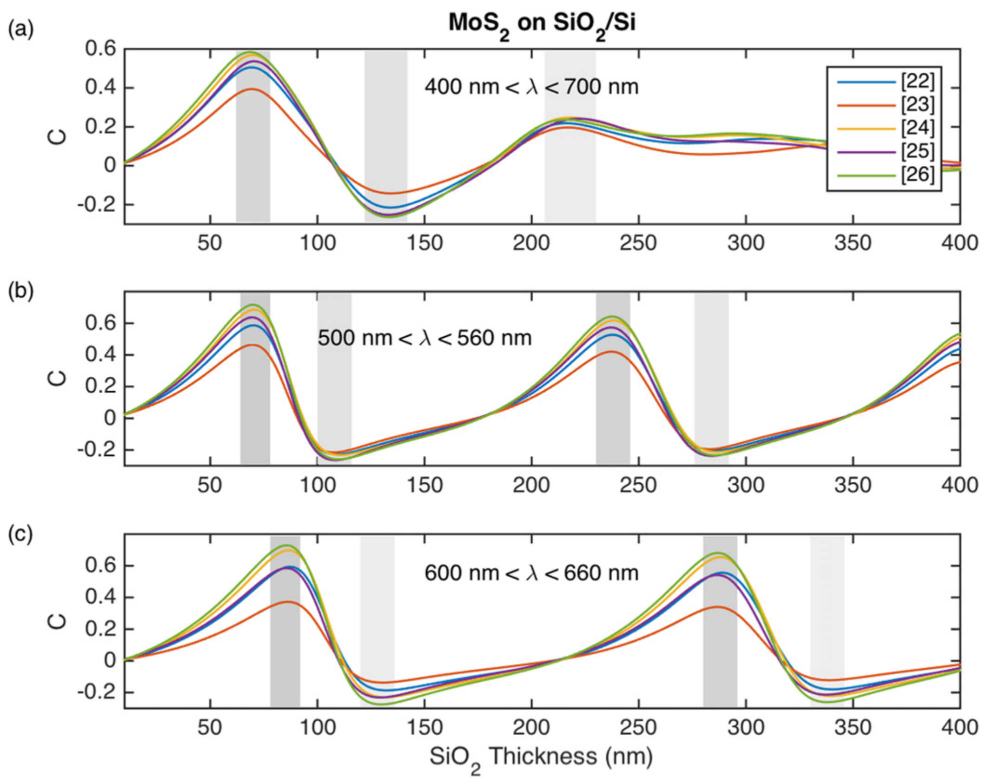

Figure 3. For MoS_2 analysis: (a)–(c) color contrast line-profile plots as a function of SiO_2 thickness for three different wavelength ranges using different MoS_2 refractive index models provided in [22–26]. The shaded bar regions correspond to the highest positive and negative contrast regions.

wavelength regions. Since there are several sets of results available for the refractive index of MoS_2 in the recent literature, we implement 5 of them in our calculations [22–26]. As shown in figure 3, the behaviors of the contrast functions all look alike; the main difference is their strengths. Since the data set provided in [22] gives almost the average of all 5, in the second set of calculations we use refractive indices reported in [22] for MoS_2, $MoSe_2$, WS_2, and WSe_2 for the optimization of d_2 parameter. Our analyzed results of contrast line-profile as a function of SiO_2 thickness are compared with reported results as shown in figures 3(a)–(c), which match well with those reported for monolayer MoS_2 material. Similar color contrast line-profiles with comparison to other reports are plotted in figures S1, S2, and S3 for monolayer $MoSe_2$, WS_2 and WSe_2, respectively. In reference [5], positive good contrast from monolayer MoS_2 can be obtained by using a 78 or 272 nm thick SiO_2 layer the when green channel (495–530 nm) of a color camera is used, whereas we suggest using a 71 ($\pm$7) nm and 238 ($\pm$8) nm thick SiO_2 layer to achieve good positive contrast at $500 \leqslant \lambda \leqslant 560$ nm. Table 2 summaries the values of underlying oxide thickness with color contrast values as a percentage at three different wavelength regions. In the case of green light, for SiO_2 thickness of 71 nm and 238 nm, the contrast is in the 55–60% range while for 108 nm and 284 nm thick SiO_2, the contrast is negative and it is ~ -22 to -25%.

To analyze ATLM buried in SiO_2 in sandwich geometry, we employ the same method discussed earlier for graphene, and we have analyzed four different types of ATLM: MoS_2, $MoSe_2$, WS_2 and WSe_2. Average color contrasts for the green wavelength range are plotted for the four ATLMs in figures 4(a)–(d). To cover different wavelength regions, the average contrasts are also plotted for all four ATLMs in red and white light ranges as shown in figures 5 and 6, respectively.

For green light filtering results of MoS_2 (figure 4(a)), we have the possibility of using two sets of d_1 values: the first set is between 43 and 70 nm and the second set is between 214

Table 2. Parameters of underlying oxide thickness with color contrast values (C) as a percentage (%) at three different wavelength regions for monolayer MoS_2 coated SiO_2/Si wafers.

	White light $400 \leqslant \lambda \leqslant 750$ nm		Green light $500 \leqslant \lambda \leqslant 560$ nm		Red light $600 \leqslant \lambda \leqslant 660$ nm	
	d_1 (nm)	C (%)	d_1 (nm)	C (%)	d_1 (nm)	C (%)
MoS_2	70 (±7)	+55	71 (±7)	+60	86 (±7)	+58
	134 (±6)	−25	108 (±8)	−25	128 (±8)	−20
	218 (±9)	+20	238 (±8)	+55	288 (±8)	+52
			284 (±7)	−22	337 (±7)	−18

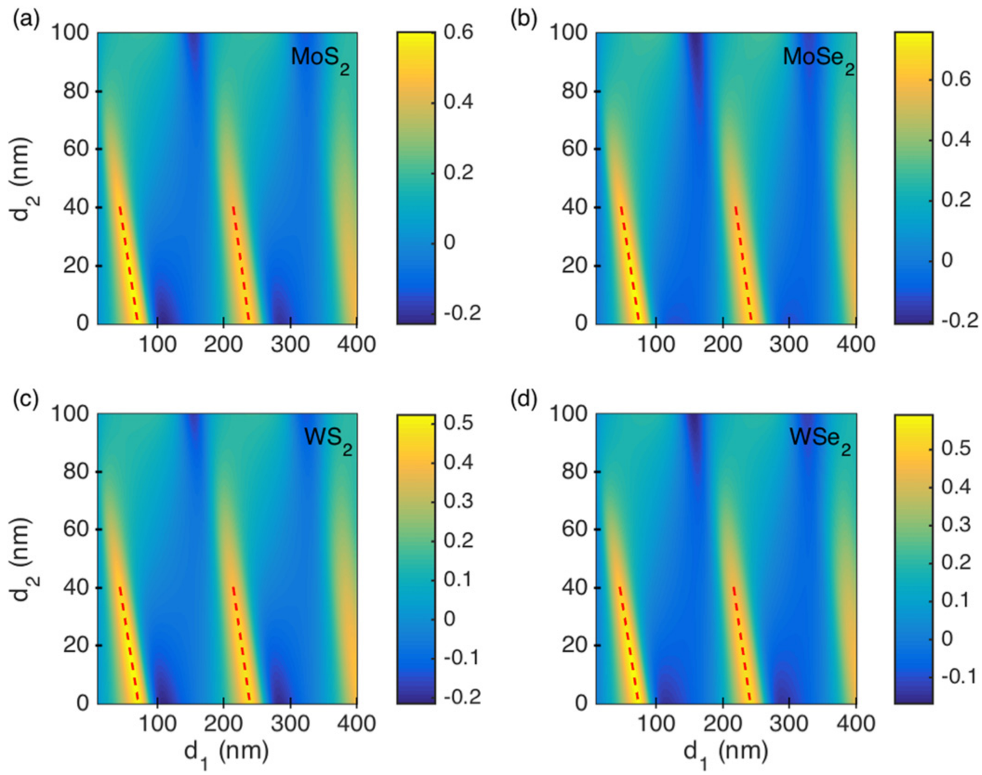

Figure 4. Color plot of the average contrast for green light ($500 \leqslant \lambda \leqslant 560$ nm) as a function of SiO_2 thicknesses (d_1 and d_2) for SiO_2/ATLM/SiO_2/Si substrates where the ATLM is (a) MoS_2 (b) $MoSe_2$, (c) WS_2, and (d) WSe_2. The color scales on the right show the expected contrasts.

and 238 nm. However, it should be noted that the second group yields a slightly smaller contrast, especially for monolayer MoS_2. Again, d_2 should not be bigger than 40 nm and the optimum d_1 value for a selected d_2 can be calculated using equation (3) with the coefficients listed in table 3. As expected, slightly bigger d_1 and d_2 values are suggested for those working with the red light region. However, the contrasts in the red channel are slightly less than the ones in the green channel. For all four ATLMs at green filtering light, the average color contrast exhibits two main characteristic bands (figures 4(a)–(d)) with high and positive values corresponding to a certain range of underlying oxide layer thickness and capping layer thickness as listed in table 3. Figures 4(a)–(d) show that, for fixed capping layer thickness (d_2), the contrast exhibits an oscillation depending on the underlying oxide layer thickness (d_1) for all four different types of ATLM and the maximum average contrast is obtained with monolayer $MoSe_2$ as compared with other ATLMs.

Table 3 presents all the suggested thickness ranges for underlying and capping SiO_2 layers in a sandwich structure geometry of SiO_2/ATLM/SiO_2/Si substrate to obtain good average color contrast at different wavelength ranges. We find that for average color contrast for various ATLM systems, the capping oxide layer thickness (d_2) should be less than or equal to 40 nm in the green channel. For example, for good and maximized contrast of ATLMs corresponding to green light in a sandwich geometry with capping thickness $d_2 = 20$ nm, the calculated values of underlying oxide thickness (d_1) are ∼56.5, ∼60.5, ∼57, ∼59 nm for MoS_2, $MoSe_2$, WS_2, and WSe_2, respectively. This study might help to make the ATLM more visible in sandwich structures on Si

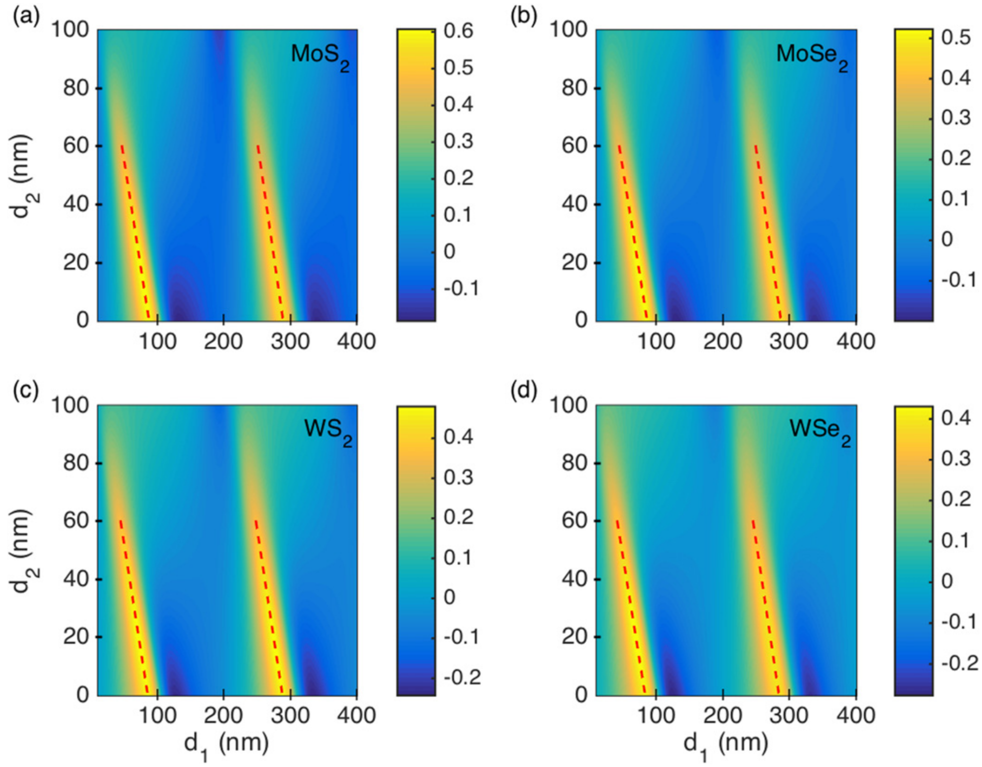

Figure 5. Same as figure 4 for wavelength range of $600 \leqslant \lambda \leqslant 660$ nm.

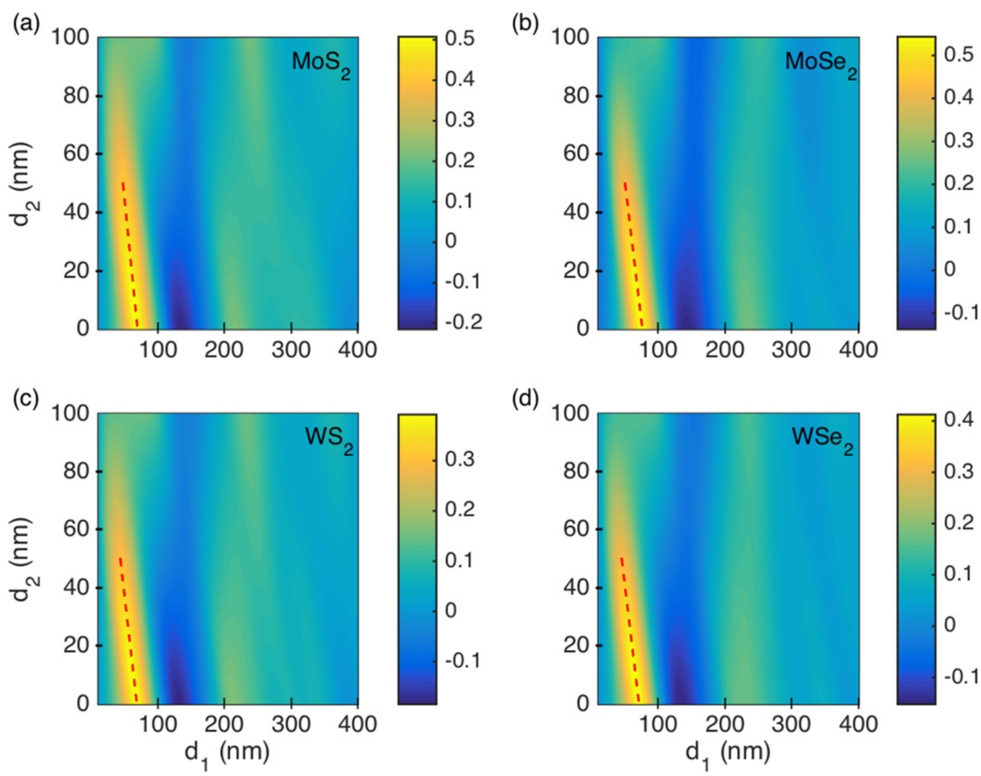

Figure 6. Same as figure 4 for wavelength range of $400 \leqslant \lambda \leqslant 750$ nm.

Table 3. Suggested d_1 ranges and equations to calculate the optimum d_2 values that maximize the visibility of ATLMs over three different wavelength ranges.

	White light $400 \leqslant \lambda \leqslant 750$ nm $0 \leqslant d_2 \leqslant 50$ nm	Green light $500 \leqslant \lambda \leqslant 560$ nm $0 \leqslant d_2 \leqslant 40$ nm		Red light $600 \leqslant \lambda \leqslant 660$ nm $0 \leqslant d_2 \leqslant 60$ nm	
MoS_2	$d_1 \approx 69 - 0.44d_2$	$d_1 \approx 70 - 0.675d_2$	$d_1 \approx 238 - 0.6d_2$	$d_1 \approx 87 - 0.683d_2$	$d_1 \approx 289 - 0.63d_2$
	$47 \leqslant d_1 \leqslant 69$ nm	$43 \leqslant d_1 \leqslant 70$ nm	$214 \leqslant d_1 \leqslant 238$ nm	$46 \leqslant d_1 \leqslant 87$ nm	$251 \leqslant d_1 \leqslant 289$ nm
$MoSe_2$	$d_1 \approx 76 - 0.52d_2$	$d_1 \approx 74 - 0.675d_2$	$d_1 \approx 243 - 0.6d_2$	$d_1 \approx 86 - 0.7d_2$	$d_1 \approx 287 - 0.63d_2$
	$50 \leqslant d_1 \leqslant 76$ nm	$47 \leqslant d_1 \leqslant 74$ nm	$219 \leqslant d_1 \leqslant 243$ nm	$44 \leqslant d_1 \leqslant 86$ nm	$249 \leqslant d_1 \leqslant 287$ nm
WS_2	$d_1 \approx 68 - 0.5d_2$	$d_1 \approx 71 - 0.7d_2$	$d_1 \approx 239 - 0.625d_2$	$d_1 \approx 85 - 0.683d_2$	$d_1 \approx 288 - 0.67d_2$
	$43 \leqslant d_1 \leqslant 68$ nm	$43 \leqslant d_1 \leqslant 71$ nm	$214 \leqslant d_1 \leqslant 239$ nm	$44 \leqslant d_1 \leqslant 85$ nm	$248 \leqslant d_1 \leqslant 288$ nm
WSe_2	$d_1 \approx 71 - 0.52d_2$	$d_1 \approx 73 - 0.7d_2$	$d_1 \approx 241 - 0.625d_2$	$d_1 \approx 83 - 0.7d_2$	$d_1 \approx 284 - 0.65d_2$
	$45 \leqslant d_1 \leqslant 71$ nm	$45 \leqslant d_1 \leqslant 73$ nm	$216 \leqslant d_1 \leqslant 241$ nm	$41 \leqslant d_1 \leqslant 83$ nm	$245 \leqslant d_1 \leqslant 284$ nm

substrates by selecting the proper incident light of a specific wavelength range.

Conclusion

In summary, we have calculated the average contrast value of different ATLMs in a sandwich geometry of SiO_2/ATLM/SiO_2/Si substrate to find the optimum oxide thicknesses for higher visibility in three different wavelength regions. Our calculations show that the thickness of the capping layer, d_2, should be less than or equal to 50, 40, and 60 nm for white, green, and red light, respectively. Furthermore the thickness of the underlying oxide can be calculated as a function of d_2 for a chosen wavelength range. These plots and the summary of our study might be useful as a benchmark and guideline of oxide/ATLM/oxide sandwich structures for both fundamental studies and device applications at different wavelength regions of the solar spectrum.

References

[1] Ferrari *et al* 2015 Science and technology roadmap for graphene, related two-dimensional crystals, and hybrid systems *Nanoscale* **7** 4598–810

[2] Chen S Y, Zheng C, Fuhrer M S and Yan J 2015 Helicity-resolved Raman scattering of MoS_2, $MoSe_2$, WS_2, and WSe_2 atomic layers *Nano Lett.* **15** 2526–32

[3] Chhowalla M, Shin H S, Eda G, Li L J, Loh K P and Zhang H 2013 The chemistry of two-dimensional layered transition metal dichalcogenide nanosheets *Nat. Chem.* **5** 263–75

[4] Blake P, Hill E W, Castro Neto A H, Novoselov K S, Jiang D, Yang R, Booth T J and Geim A K 2007 Making graphene visible *Appl. Phys. Lett.* **91** 063124

[5] Benameur M M, Radisavljevic B, Sahoo S, Berger H and Kis A 2011 Visibility of dichalcogenide nanolayers *Nanotechnology* **22** 125706

[6] Wang Y Y, Gao R X, Ni Z H, He H, Guo S P, Yang H P, Cong C X and Yu T 2012 Thickness identification of two-dimensional materials by optical imaging *Nanotechnology* **23** 495713

[7] Gomez A C, Agraït N and Bollinger G R 2010 Optical identification of atomically thin dichalcogenide crystals *Appl. Phys. Lett.* **96** 213116

[8] Li H, Wu J, Huang X, Lu G, Yang J, Lu X, Xiong Q and Zhang H 2013 Rapid and reliable thickness identification of two-dimensional nanosheets using optical microscopy *ACS Nano* **7** 10344–53

[9] Casiraghi C, Hartschuh A, Lidorikis E, Qian H, Harutyunyan H, Gokus T, Novoselov K S and Ferrari A C 2007 Rayleigh imaging of graphene and graphene layers *Nano Lett.* **7** 2711–7

[10] Roddaro S, Pingue P, Piazza V, Pellegrini V and Beltram F 2007 The optical visibility of graphene: interference colors of ultrathin graphite on SiO_2 *Nano Lett.* **7** 2707–10

[11] Zhang H, Ma Y, Wan Y, Rong X, Xie Z, Wang W and Dai L 2015 Measuring the refractive index of highly crystalline monolayer MoS_2 with high confidence *Sci. Rep.* **5** 8440 1-7

[12] Lien D H *et al* 2015 Engineering light outcoupling in 2D materials *Nano Lett.* **15** 1356–61

[13] Chen Y F *et al* 2011 Rapid determination of the thickness of graphene using the ratio of color difference *J. Phys. Chem.* C **115** 6690–3

[14] Ni Z H, Wang H M, Kasim J, Fan H M, Yu T, Wu Y H, Feng Y P and Shen Z X 2007 Graphene thickness determination using reflection and contrast spectroscopy *Nano Lett.* **7** 2758–63

[15] Mukherjee B, Leong W S, Li Y, Gong H, Sun L, Shen Z X, Simsek E and Thong J T L 2015 Raman analysis of gold on WSe_2 single crystal film *Mater. Res. Express* **2** 065009

[16] Kats M A *et al* 2013 Enhancement of absorption and color contrast in ultra-thin highly absorbing optical coatings *Appl. Phys. Lett.* **103** 101104

[17] Sercombe D *et al* 2013 Optical investigation of the natural electron doping in thin MoS_2 films deposited on dielectric substrates *Sci. Rep.* **3** 3489

[18] Lee H S, Min S W, Chang Y G, Park M K, Nam T, Kim H, Kim J H, Ryu S and Im S 2012 MoS_2 nanosheet phototransistors with thickness-modulated optical energy gap *Nano Lett.* **12** 3695–700

[19] Bao W, Cai X, Kim D, Sridhara K and Fuhrer M S 2013 High mobility ambipolar MoS_2 field-effect transistors: Substrate and dielectric effects *Appl. Phys. Lett.* **102** 042104

[20] Henrie J, Kellis S, Schultz S and Hawkins A 2004 Electronic color charts for dielectric films on silicon *Opt. Express* **12** 1464–9

[21] Simsek E 2013 A closed-form approximate expression for the optical conductivity of graphene *Opt. Lett.* **38** 1437–9

[22] Li Y *et al* 2014 Measurement of the optical dielectric function of monolayer transition-metal dichalcogenides: MoS_2, $MoSe_2$, WS_2, and WSe_2 *Phys. Rev.* B **90** 205422

[23] Mukherjee B, Tseng F, Gunlycke D, Amara K K, Eda G and Simsek E 2015 Complex electrical permittivity of the

monolayer molybdenum disulfide (MoS2) in near UV and visible *Opt. Mater. Express* **5** 447–55
[24] Shen C C, Hsu Y T, Li L J and Liu H L 2013 Charge dynamics and electronic structures of monolayer MoS_2 films grown by chemical vapor deposition *Appl. Phys. Express* **6** 125801
[25] Li S L, Miyazaki H, Song H, Kuramochi H, Nakaharai S and Tsukagoshi K 2012 Quantitative Raman spectrum and reliable thickness identification for atomic layers on insulating substrates *ACS Nano* **6** 7381–8
[26] Liu H L, Shen C C, Su S H, Hsu C L, Li M Y and Li L J 2014 Optical properties of monolayer transition metal dichalcogenides probed by spectroscopic ellipsometry *Appl. Phys. Lett.* **105** 201905
[27] Kim H C *et al* 2015 Engineering optical and electronic properties of WS_2 by varying the number of layers *ACS Nano* doi:10.1021/acsnano.5b01727
[28] Beal A R, Liang W Y and Hughes H P 1976 Kramers-Kronig analysis of the reflectivity spectra of 3R-WS_2 and 2H-WSe_2 *J. Phys. C: Solid State Phys.* **9** 2449
[29] Vuye G, Fisson S, Van V N, Wang Y, Rivory J and Abelès F 1993 Temperature dependence of the dielectric function of silicon using *in situ* spectroscopic ellipsometry *Thin Solid Films* **233** 166–70
[30] Malitson H 1965 Interspecimen comparison of the refractive index of fused silica *J. Opt. Soc. Am.* **55** 1205–8
[31] Chew W C 1999 *Planarly Layered Media in Waves and Fields in Inhomogenous Media* (New York: Wiley) ch 2